Published in final edited form as:
Dev Biol. 2012 September 15; 369(2): 235–248. doi:10.1016/j.ydbio.2012.06.023.

Hemicentin 2 and Fibulin 1 are required for epidermal-dermal junction formation and fin mesenchymal cell migration during zebrafish development

Natália Martins Feitosa[1,2,*], **Jinli Zhang**[1], **Thomas J. Carney**[3], **Manuel Metzger**[1], **Vladimir Korzh**[3], **Wilhelm Bloch**[4,5], and **Matthias Hammerschmidt**[1,2,5,‡]

[1]Institute of Developmental Biology, University of Cologne, Cologne, Germany

[2]Center for Molecular Medicine Cologne, University of Cologne, Cologne, Germany

[3]Institute of Molecular and Cell Biology, Proteos, Singapore

[4]Institute of Cardiology and Sports Medicine, German Sport University Cologne, Cologne, Germany

[5]Cologne Excellence Cluster on Cellular Stress Responses in Aging-Associated Diseases; University of Cologne, Cologne, Germany

Summary

Hemicentin 1 (Hmcn1) and Hemicentin 2 (Hmcn2) belong to the fibulin family of extracellular matrix (ECM) proteins that play pivotal roles during development and homeostasis of a variety of vertebrate tissues. Recently, we have shown that mutations in zebrafish Hmcn1, also called Fibulin 6, lead to massive fin blistering, similar to the defects caused by the Fraser syndrome gene Fras1. In contrast, the role of Hmcn2 during vertebrate development has thus far been uncharacterized. In zebrafish, *hmcn2,* like *fibulin 1 (fbln1),* another member of the fibulin family, is predominantly expressed in fin mesenchymal cells and developing somites, contrasting the strict epithelial expression of *hmcn1.* While antisense morpholino oligonucleotide (MO) – based knockdown of *hmcn2* did not yield any discernable defects, *hmcn2/fbln1* double knockdown fish displayed blistering in the trunk, pointing to an essential contribution of these proteins from mesodermal sources for proper epidermal-dermal junction formation. In contrast, and unlike *hmcn1* mutants, epidermal-dermal junctions in the fin folds of *hmcn2/fbln1* double knockdown fish were only moderately affected. Instead, they displayed impaired migration of fin mesenchymal cells into the fin folds, pointing to a crucial role of Hmcn2 and Fbln1 to remodel the ECM of the fin fold interepidermal space, which is a prerequisite for fibroblast ingrowth. TEM analyses suggest that this ECM remodeling occurs at the level of actinotrichia, the collageneous migration substrate of mesenchymal cells, and at the level of cross fibers, which resemble mammalian microfibers. This work provides first insights into the role of Hmcn2 during vertebrate development, identifying it as an evolutionary conserved protein that acts in functional redundancy with Fbln1C and/or Fbln1D isoforms to regulate tissue adhesion and cell migration, while extending current knowledge of the functions of vertebrate Fbln1.

‡Author for correspondence: mhammers@uni-koeln.de; phone: (49) 221 470 5665; fax: (49) 221 470 5164.
*present address: Universidade Federal do Rio de Janeiro - NUPEM/UFRJ, Campus Macaé, Brazil

Keywords

zebrafish; blistering; epidermal-dermal junction; fin development; fin mesenchyme; cell migration; Hemicentin; Fibulin 1

Introduction

Fibulins are secreted glycoproteins that can associate with various components of the extracellular matrix (ECM), including the basement membrane (BM) and elastic microfibers. Being involved in the elaboration and stabilization of the ECM, they have been implicated in tissue organogenesis, vasculogenesis, fibrogenesis and tumorigenesis (de Vega et al., 2009). The different members of the fibulin family share a common multimodular organization divided in three domains, with an N-terminal domain I that varies among the family members, a central domain II consisting of a variable number of epidermal growth factor (EGF)-like modules, most of which contain a consensus sequence for calcium binding (cbEFG-like modules), and the C-terminal domain III, also called Fibulin C-terminal globular (FC) domain, which is specific to the seven fibulin family members (Fibulin 1–7) (de Vega et al., 2009).

The first fibulin discovered was Fibulin1 (Fbln1) (Argraves et al., 1989; Argraves et al., 1990). Many ECM or BM proteins have been identified to bind Fibulin1, including Fibronectin, laminins, nidogens and the endostatin domain of Collagen XVIII (Balbona et al., 1992; Sasaki et al., 1998; Sasaki et al., 1995; Tran et al., 1997); but also elastic fiber components and growth factors (Perbal et al., 1999). In human, alternative splicing of *FIBULIN 1* gives rise to four different isoforms, A, B, C and D, which differ in domain III, while in other vertebrate (mouse, chicken, zebrafish) as well as invertebrate species (the nematode *C. elegans),* only Fbln1C and -1D isoforms have been described (Argraves et al., 1990; Barth et al., 1998; Pan et al., 1993; Zhang et al., 1997). *Fbln1* mutant mice lacking both Fbln1 isoforms display multiple developmental defects within blood vessels, renal glomeruli, lung alveoli and neural-crest derivatives, leading to perinatal lethality (Cooley et al., 2008; Kostka et al., 2001). To investigate the roles of the different isoforms, possibly justifying their conservation throughout metazoan evolution, splice variant-specific loss-of-function studies have been performed in *C. elegans,* re-introducing either *fbln1C* or *fbln1D* into *fbln1* -deficient mutants. These studies revealed both isoform-specific and shared functions, with a predominant requirement of Fbln1C for cell shape and adhesion regulation during tissue morphogenesis, and a specific requirement of Fbln1D to connect different tissues via flexible polymers (Muriel et al., 2005). Interestingly, however, the assembly of both Fbln1 isoforms in multiple locations is dependent upon the presence of Hemicentin (Hmcn), another member of the fibulin family also called Fibulin-6 (Muriel et al., 2005).

Like Fbln1, Hemicentins are ancient ECM proteins, with highly conserved orthologues in nearly all metazoans. While invertebrates like *C. elegans* have a single *hmcn* gene, usually two paralogues exist in vertebrates, called *Hmcn1* and *Hmcn2* (Vogel et al., 2006). With a mass of >600kDa, Hmcns are by far the largest members of the fibulin family, with multiple, evolutionary conserved modules. The most highly conserved is an amino-terminal von Willebrand A (VWA) domain, followed by a long (>40) stretch of tandem immunoglobulin (Ig) domains. The vertebrate Hemicentins have an additional G2F motif between the Ig and EGF domains. Apart from Hmcn1 and Hmcn2, this G2F domain is only found in Nidogens, where it for instance mediates binding to the BM proteoglycan Perlecan (Hopf et al., 2001). Furthermore, mammalian Hmcn1, but not Hmcn2, has a series of six thrombospondin repeats inserted between the Ig and Nidogen G2F domains (Vogel et al., 2006). In *C. elegans,* the N-terminal VWA domain is involved in pericellular Hmcn

localization, while the C-terminal Fibulin (FC) domain mediates Hmcn-Hmcn interactions as it assembles into higher order polymers (Dong et al., 2006; Vogel et al., 2006).

In *C. elegans,* Hmcn has pleiotropic functions in transient cell contacts that are required for cell migration and BM invasion, as well as for stable cell-ECM contacts at hemidesmosome-mediated cell junctions and elastic fiber-like structures (Vogel and Hedgecock, 2001; Vogel et al., 2006). In vertebrates, loss-of-function experiments have thus far only been performed for Hmcn1, but not Hmcn2. In mouse, homologous recombination of *Hmcn1* has been reported to cause early defects in cytokinesis and death of homozygous embryos at preimplantation stages (Xu and Vogel, 2011), corresponding to a similar role of Hmcn in the *C. elegans* germline (Xu and Vogel, 2011).

Recently, we have described zebrafish *hmcn1* mutants, which in contrast to the mouse mutants are viable, but display specific blistering in the developing fins (Carney et al., 2010). These defects are similar to those found in zebrafish bearing mutations in Fras1, Frem1 or Frem2 (Carney et al., 2010), BM-associated proteins which upon mutation in human cause Fraser syndrome, a recessive multisystem disorder characterized by embryonic epidermal blistering, cryptophthalmos, syndactyly, renal defects and a range of other developmental abnormalities (Smyth and Scambler, 2005). The elevating fin fold of teleosts constitutes a relatively simple yet distinctive structure, consisting of two opposing epidermal sheets, each with an underlying BM, which are attached to each other via so-called cross fibers spanning the interepidermal/dermal space between the two sheets (Dane and Tucker, 1985). In addition, the dermal space contains well-ordered arrays of collagenous actinotrichia, which run along the proximodistal axis of the elevating fin fold (Dane and Tucker, 1985). Constituents of these fibers are most likely produced by epidermal cells (Duran et al., 2011), while the dermal space is initially cell-free (Dane and Tucker, 1985). Only later, it is invaded by fibroblast-like fin mesenchymal cells that use the actinotrichia as migration substrate (Wood and Thorogood, 1984). Like *fras1* and most other ECM component-encoding genes, *hmcn1* is expressed in apical-most epidermal cells of the elevating fin fold, while *fras1* and *hmcn1* mutants display compromised epidermal-dermal junction formation, with blisters directly underneath the BM (Carney et al., 2010). In contrast, *hmcn2* shows prominent expression in the invading fin mesenchymal cells (Carney et al., 2010), whose biology and role during fin morphogenesis is poorly understood.

Here, we report that of all zebrafish fibulin family members, *fbln1* and *hmcn2* are co-expressed in fin mesenchymal cells and in somitic muscle progenitors. Morpholino-based knockdown of *fbln1* causes defects during the formation of intersomitic blood vessels, while *hmcn2* knockdown does not lead to any discernible defects, nor does it enhance the fin blistering of *hmcn1* mutants. However, concomitant loss of both *fbln1* and *hmcn2* leads to compromised epidermal-dermal attachment at somite levels, and to compromised migration of fin mesenchymal cells through the dermal space of the fin folds. Results obtained with specific splice-blocking morpholinos and via rescue experiments further indicate that Fbln1C and Fbln1D can compensate for each other during epidermal-dermal junction formation, but not during mesenchymal cell migration. This work represents the first functional analysis of Hmcn2 function in any vertebrate species, and unravels thus far unappreciated redundant roles between Fbln1 isoforms and Hemicentins, which are required both for ECM junction formation and for ECM remodelling to allow proper mesenchymal cell migration.

Materials and Methods

Fish lines and handling

Fish lines used in this project were TL/EK (wild type), the transgenic enhancer trap line ET37 (Choo et al., 2006), and the transgenic line *Tg(fli1a:EGFP),* labelling blood vessels (Lawson and Weinstein, 2002). Embryos and larvae were kept at standard conditions (28°C) and staged in hours post fertilization (hpf) as described (Kimmel et al., 1995).

Morpholinos, efficacy controls, and mRNA rescues

Morpholino oligonucleotides (MOs) were purchased at Gene Tools, LLC. 1 mM stock solutions in distilled water were prepared and aliquots stored at −20°C. Before use, morpholinos were preheated at 70°C for 10 minutes, diluted in Danieau's buffer and phenol red (0,05%) (Sigma) to indicated concentrations (Table 1), and microinjected into 1-4 cell stage embryos (1.5 nl per embryo) as described (Nasevicius and Ekker, 2000). As negative control, standard morpholino (std MO) was obtained from Gene Tools, LLC. The morpholinos used were:

fbln1-atg-1: ACAACACGATCATGTAGAGATCCAT

fbln-atg-2: ATTATCCAGACGCTGGAGTGTTTAT

fbln1c-splice: CGGCTGCAGACGCACACAAGAAGAC

fbln1d-splice: GTCTGCTAGAGGAATGACACACAAT

hmcn2-atg-1: TAACGACAAACTTTTTCATTCTCAC

hmcn2-atg-2: CTCACTTTAAATTCATTAGCTCACT

Data obtained with *hmcn2-atg-1* MO are shown. However, for all studies, both *hmcn2* MOs were used and gave identical results in at least three independent experiments. The same applies to the two *fbln1-atg-1* and *fbln-atg2* MOs.

For efficacy control of the *fbln1-atg* MOs, an Fbln1-GFP constructs was generated as follows: cDNA of zebrafish embryos was synthesized with Superscript III 1st strand (Invitrogen) according to the manufacturer's protocol. The 5′ region of *thefbln1* cDNA was amplified by PCR with primers containing *Eco*RI or *XbaI* the restriction sites. After restriction digest, the PCR fragment was cloned into XLT.GFP$_{LT}$ CS2+. The resulting *fbln1*-XLT.GFP$_{LT}$ CS2 plasmid contained the SP6 promoter, *thefbln1* 5′UTR and 195bp of *flbn1* coding region fused in frame to the GFP (Green Fluorescent Protein) coding region. Capped sense mRNAs from XLT.GFP$_{LT}$ CS2 *(GFP* control) and *fbln1*-XLT.GFP$_{LT}$ CS2 were synthesized using the MEGA script kit (Ambion).

For morphant rescue experiments, mouse *Fbln1C* plasmid IRAVp968A0213D (Imagenes GmbH; GenBank number BC007140; 2.22kb) was linearized with *NotI* and capped mRNA was synthesized with Sp6 RNA polymerase. For synthesis of capped mouse *Fbln1D* mRNA, plasmid I420027B09, (Imagenes GmbH; GenBank AK159646; 2.69kb) was linearized with *KpnI* and transcribed with T7 RNA polymerase, using the Message Machine kit (Ambion). mRNAs were co-injected with morpholinos after dilution in distilled water/phenol red at indicated concentrations (Table 1; 1.5 nl per embryo).

For efficacy control of *fbln1c-splice* and *fbln1d-splice* MOs, semi-quantitative RT-PCR of RNA isolated from embryos (24 hpf) injected with either of the two MOs was carried out, using the following primers and PCR conditions: *flbn1c/d* forward: GAGTGTCTGACGGGGACTCA; *fbln1c* reverse: CATGCGGAAGAGGTCAGTG; *fbln1d* reverse: TCTGAAGGTGGGTAGGGAGA. Loading control: *ef1*α forward:

TCACCCTGGGAGTGAAACAGC; *ef1α* reverse: ACTTGCAGGCGATGTGAGCAG. Annealing temperature: 57°C; 30 cycles.

Cell transplantations

Wild-type embryos were injected either with rhodamin dextran (RD; 10 kDa; 50mg/ml) or with RD + *hmcn2* MO *+fbln1MO.* At the shield stage (6 hpf), cells were collected from the ventral side of injected donors and transplanted into the same side of either un-injected ET37 hosts of the same stage, or into ET37 hosts injected *hmcn2* and *fbln1MOs.* Chimeric embryos were evaluated at 72 hpf via confocal microscopy.

In situ hybridization

Embryos were fixed in 4% PFA overnight at 4°C, and in situ hybridizations were performed as previously described (Hammerschmidt et al., 1996) with RNA probes generated from linearized plasmids using the Roche digoxygenin RNA synthesis kit. For *fibulin1–5,* plasmid *pSport-zffbln1* (MPMGp609N1134) with a 1.7 *kbfbln1* cDNA fragment was linearized with *Sal*I and transcribed with SP6 RNA polymerase, plasmid *pBluescriptSK-zffbln2* (recloned from IMAGp998B086485Q) with a 1.8 kb *fbln2* cDNA fragment was linearized with *Eco*RI and transcribed with T3 RNA polymerase, plasmid *pExpress1-zffbln3* (IMAGp998D1614790Q) with a 3.5 kb *fbln3* cDNA fragment was linearized with *Eco*RI and transcribed with T7 RNA polymerase, plasmid *pBluescriptSK-zffbln4* (recloned from IRBOp991B0954D) with a 1.8 kb *fbln4* cDNA fragment was linearized with *Eco*RI and transcribed with T3 RNA polymerase, plasmid *pExpress1-zffbln5* (IMAGp998A0619304Q) with a 1.5 kb *fbln5* cDNA fragment was linearized with *Eco*RI and transcribed with T7 RNA polymerase. For *hmcn1* and *hmcn2,* 0.75 kb and 1.0 kb cDNA fragments, respectively, were amplified from zebrafish RNA via RT-PCR and cloned into pGEMT-easy (Promega). For *hmcn1* probe, plasmid *pGEMT-hmcn1* was linearized with *NotI* and transcribed with SP6 RNA polymerase, for *hmcn2* probe, *pGEMT-hmcn2* was linearized with *Sac*II and transcribed with SP6 RNA polymerase.

Generation of polyclonal anti-Hmcn2 antibody

A cDNA construct encoding amino acid residues 34 – 425 of zebrafish Hemicentin 2 was generated by RT-PCR on total RNA from 24 hpf embryos and cloned with 5′-terminal *NheI* and 3′-terminal *XhoI* restriction sites. The amplified PCR product was inserted into a modified pCEP-Pu vector containing an N-terminal BM-40 signal peptide and a C-terminal strepII-tag downstream of the restriction sites (Maertens et al., 2007). The recombinant plasmid was introduced into HEK293-EBNA cells (Invitrogen) using FuGENE 6 transfection reagents (Roche). Cells were selected with puromycin (1 μg/ml) and the recombinant protein was purified directly from serum-containing cell culture medium. After filtration and centrifugation (30 min, 10,000 × *g*), cell culture supernatants were applied to a Streptactin column (1.5 ml, IBA GmbH) and eluted with 2.5 mM desthiobiotin, 10 mM Tris–HCl, pH 8.0. The purified recombinant Hmcn2 fragment was used to immunize a rabbit (Pineda Antikörper Service, Berlin, Germany). Obtained antisera were purified by affinity chromatography on a column with purified Hmcn2 fragment coupled to CNBr-activated Sepharose (GE Healthcare). Specific antibodies were eluted with 3M KSCN, and the eluate was dialysed against PBS, pH7.4.

Immunohistochemistry

Whole mount immunostainings were done according to (Schulte-Merker et al., 1992) with minor changes (washes in PBS + 0,05% Tween20). The antibodies used and their dilutions were: rabbit anti-zebrafish Hmcn2 (1:50), rabbit anti-laminin (1:200, Sigma L9393), mouse anti-p63 (1:200, Santa Cruz A4A), goat anti-rabbit Cy3 (1:200, Invitrogen A10520),

AlexaFluor488 goat anti-rabbit (1:200, Invitrogen A11008). In the case of Phalloidin-cy3 (1:200) staining, samples were washed in PBST after fixation and immersed in water, followed by the regular immunostaining protocol. For counterstaining of nuclear DNA, immunostained embryos were incubated in DAPI solution for 10 minutes and post-fixed with 4% PFA in PBS. Afterwards, embryos were embedded in Durcupan and sectioned at 7μm as described in (Feitosa et al., 2011) or mounted for microscopy analysis.

Microscopy

For imaging, live embryos were anesthetized with Tricaine and mounted in 1% methyl cellulose, and embryos stained by *in situ* hybridization were mounted in 2:1 solution of benzylbenzoat: benzylalcohol (Nüsslein-Volhard and Dahm, 2002). Fluorescent images and time-lapse movies were taken with a Zeiss Confocal microscope (LSM710 META). For the time-lapse recordings, anesthetized embryos were immobilized in 1,2% low melting agarose and pictures were taken every 5 minutes for 5 hours. Bright-field or Nomarski microscopy was performed on a Zeiss Axioimager. Transmission electron microscopy (TEM) was carried out as previously described (Feitosa et al., 2011).

Results

hmcn2 and *fbln1* are co-expressed in somites and fin mesenchymal cells

According to the zebrafish genome project (http://www.ensembl.org/Daniorerio/Info/Index), the zebrafish has two *hemicentin (hmcn)* genes. One of them, *hmcn1,* located on chromosome 20 and mutated in *nagel* mutants (Carney et al., 2010), encodes a protein of 5615 amino acid residues and a domain composition identical to mammalian Hmcn1 proteins, with an N-terminal VWA domain, 44 Ig domains, 6 TSR domains, one G2F domain, 8 EGF-like domains and a C-terminal FC domain (Supplementary Fig. S1A). The predicted protein encoded by the second *hmcn* gene (GenBank accession number XM_001920466.2), located on chromosome 8, is slightly smaller (4211 aa), with a VWA domain followed by only 32 Ig domains, one TSR domain, one G2F domain, 8 EGF-like domains and one FC domain (Gene bank accession number XP001920501.2). These numbers of Ig and TSR domains are different from those of both mammalian Hmcn1 (44x Ig, 6x TSR, 8x EGF-like domains) and mammalian Hmcn2 (42/43x Ig, no TSR, 6x EGF-like domains) (Supplementary Fig. S1A). However, phylogenetic tree analysis with Hmcn1 and Hmcn2 proteins from different species (Supplementary Fig. S1B) and conservation of synteny at the genomic level (Supplementary Fig. S2) clearly indicate that this second zebrafish *hmcn* gene is a *hmcn2* orthologue, rather than a second *hmcn1* gene. This phylogenetic analysis further indicates that the vertebrate *Hmcn1* genes are the orthologues of the single invertebrate *hmcn* gene, while the vertebrate *Hmcn2* genes are more diverged.

As reported previously (Carney et al., 2010), *hmcn1* shows prominent expression in apical-most epidermal cells of the emanating median fin folds (Fig. 1B,C). *hmcn2* is expressed in the same cells, however, at much lower levels and more transiently, with expression vanishing between 24 and 48 hours post fertilization (hpf) (Carney et al., 2010), the time when strong *hmcn2* expression becomes visible in mesenchymal cells migrating into the dermal space of the median fin folds (Fig. 1E,F). In addition, in contrast to *hmcn1* (Fig. 1A), *hmcn2* shows strong expression in developing somites of trunk and tail (Fig. 1D).

To study Hmcn2 protein distribution, we generated polyclonal antibodies against zebrafish Hmcn2 (see Materials & Methods). Whole mount immunohistochemistry (IHC) and subsequent sectioning revealed Hmcn2 at myosepta between individual somites (Fig. 1J,L), and, at lower levels, surrounding the somites in the limits of the overlying skin and the neural tube (Fig. 1L). Furthermore, at later stages, Hmcn2 was present in subepidermal

regions of the developing median fins (Fig. 1M), consistent with the expression pattern determined via *in situ* hybridization. This indicates that Hmcn2 protein is secreted from cells and associated with BMs or other components of the ECM.

For loss-of-function experiments, we designed two sequence-independent antisense morpholino oligonucleotides (MOs) directed against the translational start site *(hmcn2-atg-1* MO, *hmcn2-atg-2* MO). Embryos injected with either of the two *hmcn2* MOs lacked specific anti-Hmcn2 immunolabelling (Fig. 1K; and data not shown), indicating that both work efficiently. However, neither of the two morpholinos yielded any discernable morphological defects (data not shown), suggesting that Hmcn2 function per se is dispensable for zebrafish development.

In *C. elegans,* Hmcn protein has been shown to move rather long distances within the ECM (Vogel and Hedgecock, 2001; Vogel et al., 2006). Therefore, we speculated that despite their differential expression pattern, *hmcn2* might share functions with *hmcn1.* However, co-injection of *hmcn1* and *hmcn2* MOs, or injection of *hmcn2* MOs into *nagel/hmcn1* mutants (Carney et al., 2010) did not increase the phenotypic strength or penetrance of the fin blistering defects of *hmcn1* morphants/*nagel* mutants (data not shown), suggesting that Hmcn2 does not act in partial redundancy with its direct paralogue.

As a first step to study whether Hmcn2 might act redundantly with other members of the Fibulin family, we carried out comparative *in situ* hybridization analyses between *hmcn2, fbln1, fbln2, fbln3, fbln4* and *fbln5.* Notably, of all tested five fibulin genes, only *flbn1* showed co-expression with *hmcn2* both in the somites and in the fin mesenchymal cells (Fig. 1G–I), whereas *fbln1* expression was absent in apical epidermal cells of the fin folds, the site of transient *hmcn1* and *hmcn2* co-expression (data not shown). In contrast, none of the *other fbln* genes was expressed in fin mesenchymal cells, while only *fbln4* was also expressed in somites (Supplementary Fig. S3; and data not shown).

Concomitant inactivation of *hmcn2* and *fbln1* leads to compromised epidermal-dermal junction formation in the trunk

Zebrafish *fbln1* has been previously shown to be expressed in somites, fins and other embryonic structures, including the heart valves (Zhang et al., 1997), however, functional analyses have been missing thus far. We designed two sequence-independent *fbln1* translation-blocking MOs, both of which fully suppressed translation of co-injected mRNA containing the 5′ region of *fbln1,* including the translation initiation sequence complementary to the MOs, fused to the GFP coding sequence (Supplementary Fig. S4C,D; and data not shown). *fbln1* morphant embryos, while morphologically grossly normal, displayed alterations in the patterning and integrity of intersomitic vessels (Supplementary Fig. S4A,B), pointing to a role of Fbln1 generated by somitic cells in governing angiogenesis, and consistent with the described role of Fbln1 in blood vessel formation in the mouse (Cooley et al., 2008; Kostka et al., 2001). Distinct and more striking defects were obtained upon co-injection of *hmcn2* (0.5 mM) and *fbln1* (0.1 mM) MOs in all possible combinations *(hmcn2-atg-1* + *fbln1-atg-1; hmcn2-atg-1* + *fbln1-atg-2; hmcn2-atg-2* + *fbln1-atg1; hmcn2-atg-2* + *fbln1-atg-2),* whereas none of these traits was obtained when either of the MOs was co-injected with the standard control MO. At 24 hpf, *hmcn2/fbln1* double morphants displayed massive blistering of the skin in the trunk and tail region covering the somites (Fig. 2A,B). Trunk blisters were also apparent at 48 hpf (Fig. 2C,D), but started to disappear during further development (Supplementary Fig. S5C,E). We do not know the reason for the later healing of the blisters, however, similar phenomena are observed for the transient embryonic skin blistering caused by mutations in other ECM proteins, such as Fras1, both in zebrafish (Carney et al., 2010) and in mouse (McGregor et al., 2003; Vrontou et al., 2003).

In light of data obtained in *C. elegans* pointing to both shared and isoform-specific roles of the alternative splicing variants Fbln1C and Fbln1D (see Introduction; (Muriel et al., 2005), we carried out co-injections of *hmcn2* MOs with MOs blocking Fbln1C or Fbln1D splicing. These morpholinos were designed according to genomic sequences from the trace archives of the *Danio rerio* genome. The zebrafish Fbln1C and 1D proteins share the first 541 amino acid residues, whereas the C-terminal 98 (Fbln1C) or 140 (Fbln1D) aa residues, respectively, are distinct (Zhang et al., 1997). Specific and efficient abrogation of *fbln1C* or *fbln1D* splicing in embryos injected with *fbln1c*-splice MO or *fbln1d*-splice MO, respectively, was revealed by semi-quantitative RT-PCR analysis (Supplementary Figure S6). Strikingly, embryos co-injected with *hmcn2* MO and *fbln1C MO,* or co-injected with *hmcn2* MO and *fbln1D* MO lacked trunk blisters, whereas embryos co-injected with all three MOs displayed trunk blisters at a strength and penetrance as embryos co-injected with *hmcn2* MO and a translation-blocking *fbln1* MO (Fig. 2E,F; Table 1). Consistently, the blistering defects of *fbln1-atg/hmcn2* double morphant embryos (47/75; 63%) could be significantly alleviated upon co-injection with synthetic mRNA encoding either mouse Fbln1C (20/96; 21%) or mouse Fbln1D (12/76; 16%). Together, this indicates that during epidermal-dermal junction formation, Flbn1C and Flbn1D act in functional redundancy to Hmcn2 and to each other.

To analyze the trunk blisters of *hmcn2/fbln1* double morphants in more detail, we carried out IHC and transmission electron microscopy (TEM) studies. Anti-Laminin IHC at 28 hpf (Fig. 3A,B) revealed that blisters occurred within the space between the forming BM underlying the epidermis and the BM surrounding the somites. Consistent results were obtained via TEM. During the first 5 days of development of wild-type fish, the dermal space is largely acellular, with rather scarce fibroblast-like cells called dermal endothelial cells and some melanocytes (Le Guellec et al., 2004). During these stages, dermal ECM components such as type I Collagens are mainly generated by epidermal cells, while dermal fibroblasts only immigrate later (Le Guellec et al., 2004). At 30 hpf, first collagen fibrils are visible underneath the epidermal BM (Fig. 3D), which later obtain a multi-layered plywood-like organization (Fig. 3F). *hmcn2/fbln1* double morphants displayed a rupture of dermal integrity within the first layers of collagen fibers below the BM (Fig. 3E,G). The resulting blisters initially appeared rather clear, suggesting that they are filled with fluid (Fig. 3E), whereas later on almost all of them were filled with more electron-dense, amorphic material (Fig. 3C,I), intermingled with patches of disorganized collagen fibers (Fig. 3I). In wild-type fish, such amorphic material was rarely observed and at sites with wide subepidermal spaces, such as at the base of the fins. At these locations, collagen fibers remained organized and positioned distal of the amorphic material (Fig. 3H), in contrast to the double morphant (Fig. 3I).

Together this suggests that Hmcn2 and Fbln1, generated by somites are secreted into the dermal space between somites and surrounding epidermis and contribute to proper attachment of epidermal-derived collagen fibers below the epidermal BM, and thereby proper epidermal-dermal junction formation.

In contrast to the trunk, formation of epidermal-dermal junction in the fin folds of *hmcn2/fbln1* double morphants was rather normal. As the dermis of the trunk, the dermal (interepidermal) space of the fin fold is initially cell-free, with fibroblast-like mesenchymal cells only immigrating towards the end of the second day of development (see below). Fibers consisting of Collagen I and Collagen II (Duran et al., 2011) form large parallel bundles called actinotrichia, which run along the epidermal BM (Fig. 3J). *hmcn2/fbln1* displayed rather moderate, late and locally restricted dissociation of actinotrichia from the epidermal BM (Fig. 3K). This is in striking contrast to the situation in *hmcn1* mutants, in which the epidermal-dermal junction is severely compromised from much earlier stages

onwards and along the entire length of the fin fold (Carney et al., 2010). This points to a predominant role of Hmcn1 over Hmcn2 during epidermal-dermal junction formation in the fins, consistent with the stronger and more persistent expression of *hmcn1* in the apical epidermal cells (see above).

hmcn2/fbln1 double morphants display compromised fin mesenchymal cell migration

Actinotrichia of the fin folds have structural functions, as keeping the fin fold straight (Duran et al., 2011; Zhang et al., 2010). In addition, they guide the migration of invading mesenchymal cells within the fold (Wood and Thorogood, 1984). The exact function of these mesenchymal cells is still a matter of debate, but they seem to stabilize the larval fins as well as contributing to actinotrichia and to the later formation of lepitotrichia, the bony fin rays (Duran et al., 2011; Zhang et al., 2010). During their immigration, zebrafish fin mesenchymal cells display strong expression of *hmcn2* and *fbln1* (see above), while *hmcn2/fbln1* double morphants had striking defects in fin mesenchymal cell morphology and migration behavior (Figs. 4 and 5). In contrast to trunk blistering, these defects were not only obtained upon co-injection of *hmcn2* MO and translation-blocking *fbln1* MO targeting both Fbln1C and Fbln1D, but also upon co-injection of *hmcn2* MO with either the *fbln1C* or the *fbln1D*-specific MO (Table 1), indicating that here, both Fbln1 isoforms are essential Hmcn2 partners. Although defects were visible via light microscopy (Supplementary Fig. S5D,F), for direct in vivo imaging of fin mesenchymal cells (Fig. 4), we took advantage of the transgenic enhancer trap line ET37, in which fin mesenchymal cells express GFP (Choo et al., 2006). At 55 hpf, fin mesenchymal cells of wild-type embryos radiated from basal to apical and were highly arborized, with many projections extending apically (Fig. 4A,B). In contrast, fin mesenchymal cells of *hmcn2/fbln1* double morphants agglomerated in basal regions of the fin and had a more roundish shape, with fewer and less extended projections (Fig. 4C,D).

The shape of the mesenchymal cells in *hmcn2/fbln1* double morphants resembled that of wild-type cells at an earlier developmental stage and in basal-most positions of the fin, when they initiate their migratory process (Wood and Thorogood, 1984). Two sets of results indicate that altered cell shape and failed mesenchymal migration in *hmcn2/fbln1* double morphants are not due to intrinsic deficits of mesenchymal cells themselves (e.g. the incapability to form cellular protrusions via rearrangement of the actin cytoskeleton), but to problems in the extracellular environment. First, time-lapse studies from 35 – 40 hpf in the ET37 background revealed that fin mesenchymal cells of *hmcn2/fbln1* double morphants were able to form cellular protrusions of reasonable lengths (Fig. 3F). However, compared to wild-type embryos (Fig. 3E), these protrusions were less persistent, and often retracted without an concomitant apical displacement of the cell body. Second, analysis of chimeric embryos generated by transplantation of wild-type cells into *hmcn2/fbln1* double morphant hosts during gastrula stages revealed that wild-type cells in a *hmcn2/fbln1* double morphant environment failed to migrate and behave like *hmcn2/fbln1* double morphant neighbors (Fig. 4G). Conversely, *hmcn2/fbln1* double morphant mesenchymal cells in a wild-type environment showed normal cell morphology and migration behaviour (Fig. 4H). This indicates that Hmcn2 and Fbln1 act in a non-cell autonomous manner, suggesting that mesenchymal cells secrete the proteins to “condition” the ECM for proper cell migration not just in a pericellular fashion, but also affecting at least adjacent fin mesenchymal cells.

hmcn2/fbln1 double morphants display disorganization of the fin fold ECM

To elucidate possible changes within the fin fold ECM that may cause compromised mesenchymal cell migration, we performed TEM. Consistent with the aforementioned ET37 transgenic analyses, cell bodies of mesenchymal cells were only found in basal fin fold regions of *hmcn2/fbln1* double morphants (Fig. 5B). Furthermore, while in control embryos,

cellular protrusions of fin mesenchymal cells were aligned to the actinotrichia (inset of Fig. 5A; Fig. 5G), protrusions in *hmcn2/fbln1* double morphants were usually found in more central regions of the dermal space and remote from the actinotrichia (Fig. 5F), although actinotrichia themselves appeared normal (compare Fig. 5D,F with Fig. 5E,G). In addition, we observed striking changes in the organization of the cross fibers. It was shown earlier these cross fibers are present in apical-most regions of the fin fold, spanning the subepidermal space at right angles to the actinotrichia, whereas they could not be detected in more medial and basal regions of the fin fold, leading to the speculation that they need to be eliminated to leave a clear path for the invasion of fin mesenchymal cells (Dane and Tucker, 1985). In line with these studies, we found cross fibers spanning the dermal space in apical regions of wild-type fin folds (Fig. 5C). However, cross fibers were also found in medial regions of wild-type fins, where they displayed a different spatial organization, forming bouquet-like structures in regions close to the BM and actinotrichia, while being covered with dense granular material in more interior regions of the dermal space (Fig. 5E,G). They did not seem to hinder protrusions of invading fin mesenchymal cells, which wove between them (Fig. 5G). In contrast, cross fibers of the apical organization, spanning the entire space in an unbundled and less decorated manner, were also present in medial and basal positions of *hmcn2/fbln1* double morphant fin folds (Fig. 5D,F,H), in line with the strongly reduced width of the dermal space (Fig. 5B). Furthermore, cellular protrusions of fin mesenchymal cells seemed incapable of avoiding cross fibers, but were tightly attached to them both in medial-basal regions (Fig. 5F; thin protrusion) and in basal regions (Fig. 5H; thick protrusion) of the fin fold. Together, this suggests that Hmcn2 and Fbln1 have a positive effect on the association between fin mesenchymal cells and actiontrichia, but a negative effect on the association between fin mesenchymal cells and cross fibers, so that in their absence, fin mesenchymal cells cannot follow their normal track along the actinotrichia, but get trapped within the the cross fibers. Their non-cell autonomous mode of action (see above) further suggests that this is not achieved by modulating cell surface properties of fin mesenchymal cells and their protrusions, but by modifying the ECM. In agreement with this latter notion, alterations in cross fiber organization were also seen in medial regions of wild-type fin folds, which were not reached by fin mesenchymal cell protrusions as yet (Fig. 5E).

Discussion

Hemicentin was initially discovered and functionally characterized in the nematode *C. elegans,* based on *hmcn* loss-of-function mutants in the *him-4 (high incidence of male progeny-4)* locus (for review, see (Vogel et al., 2006). Sex distortion among the self-progeny of hermaphrodites is caused by incorrect chromosome segregation in the *C. elegans* germline, in the case of *him-4 (hmcn)* mutants due to cytokinesis failures in germ cells (Vogel et al., 2011; Xu and Vogel, 2011). Interestingly, similar cytokinesis problems were observed in *Hmcn1* mutant mice during preimplantation stages, pointing to an evolutionary conserved role of these extracellular proteins to promote cleavage furrow maturation and contractile ring formation during cytokinesis (Xu and Vogel, 2011). However, *C. elegans him-4/hmcn* mutants have other developmental defects, mainly affecting adhesion and cell migration processes (Vogel and Hedgecock, 2001; Vogel et al., 2006). This work reveals comparable defects caused by concomitant loss of Hmcn2 and Fbln1 function during vertebrate development.

Hemincentins and adhesion

In *C. elegans,* Hmcn regulates adhesion across BMs separating two adjacent tissues, with distances between the two opposing BMs ranging from 100 nanometers to up to several micrometers (Vogel and Hedgecock, 2001; Vogel et al., 2006). Immunohistochemistry further revealed that Hmcn is positioned between the BMs (Vogel and Hedgecock, 2001;

Vogel et al., 2006), suggesting that it promotes tissue-tissue adhesion by regulating the anchorage between the BMs associated with each of the tissues/cells. We demonstrated a similar function for Hmcn1 during median fin formation in the zebrafish (Carney et al., 2010). At the relevant stages, the fin fold consists of two opposing epidermal sheets, both with underlying BMs, while the interepidermal space is cell free (see Fig. 6). *hmcn1* mutants display normal attachment between the basal epidermal layers and their BMs, whereas the connection between the BMs and the subepidermal space (or the connection between the two opposing epidermal BMs) is disrupted, leading to massive blistering below the BMs (Carney et al., 2010). Data presented in this work point to a similar function for Hmcn2, the more diverged Hcmn paralogue only present in vertebrates, mediating the attachment between the trunk epidermis and the somites (Figs. 2 and 3). Also here, both the epidermis and the somites are surrounded by BMs, with a largely acellular dermal space in between, while Hmcn2 plays an important role in properly connecting epidermis and somites across the dermal space. Unlike Hmcn1 in the fin fold, however, Hmcn2 is not made by epidermal cells, but by somitic cells (Fig. 1), indicating that Hmcn proteins can come from either epidermal or inner cells to establish proper tissue linkeage via their respective BMs.

In the fin fold, anchorage between the two epidermal sheets and their respective BMs has been proposed to be accomplished by cross fibers, which at least in apical-most regions of the fold span the entire interepidermal space, penetrate the BMs and terminate in direct contact with the epidermal cell membranes (Dane and Tucker, 1985) (Fig. 5C,G). The molecular composition of these cross fibers is unknown. According to our TEM analyses, they have a diameter of 10–15 nanometers, similar to mammalian microfibers, which consist of polymerized Fibrillin proteins organized in a head-to-tail arrangement (Ramirez and Sakai, 2010). Intriguingly, loss of *fibrillin2 (fbn2)* function in zebrafish leads to fin blistering similar to that of *hmcn1* mutants (Carney et al., 2010; Gansner et al., 2008b), while partial loss of Fbn2 and Hmcn1 synergistically enhance each other (Carney et al., 2010). Furthermore, cross fibers are not properly attached to the BMs in *hmcn1* mutants (Carney et al., 2010). Hence it is tempting to speculate that zebrafish Hmcn1 is involved in the anchorage of Fibrillin 2-containing cross fibers. Cross fiber-like structures might also be present in the dermal space between epidermis and somites (see Fig. 3 and its legend). Furthermore, *hmcn2, fbln1* and *fbn2* are co-expressed in somites, and *fbn2* mutants display blisters in the trunk (Gansner et al., 2008b), as do *hmcn2/fbln1* double morphants, suggesting that similar molecular systems might be at play in the subepidermal space of both the fin fold and the trunk to account for proper epidermal-dermal junction formation. Of note, trunk blisters of *hmcn2/fbln1* double morphants occur shortly after melanocytes have migrated into the dermal space (see Fig. 3D,F), suggesting that blister formation is reinforced by mechanical stress caused by cell immigration. In addition, *fbln1,* but not *hmcn2,* is also expressed in premigratory neural crest (Zhang et al., 1997), the embryonic source of melanocytes, raising the possibility that a combinatorial supply of these ECM molecules by somites and melanocytes might contribute to proper dermal ECM reorganization during and after cell immigration.

Hemicentins and cell migration

An essential positive function of Hmcn during migratory processes has thus far only been described in the nematode *C. elegans* (Sherwood, 2006; Sherwood et al., 2005; Vogel et al., 2006), while a human cell model for epithelial breast cell invasion revealed *HMCN2* as one of the genes most strongly up-regulated in invasive cells (Moon et al., 2008). Furthermore, for Fibulin 1, both positive and negative effects on cell migration have been reported in mammals and worms (Twal et al., 2001; Kubota et al., 2004; Cooley et al., 2008).

Here, we demonstrate an essential and positive role of Hmcn2 and Fbln1 on the immigration of fin mesenchymal cells into the zebrafish fin fold (Figs. 4 and 5; for schematic summary,

see Fig. 6). Invading mesenchymal cells display strong *hmcn2* expression (Fig. 1F) and secrete Hmcn2 protein into the interepidermal space where it becomes localized between epidermis and mesenchymal cells/protrusions (Fig. 1M). This is the region that contains the BMs and the actinotrichia, thick collagenous bundles positioned directly underneath the BMs, which span the fin folds in a proximodistal orientation. During normal development, the protrusions of migrating fin mesenchymal cells tightly attach to the inner surface of these actinotrichia (Figs. 5A,G and 6), suggesting that the actinotrichia act as their migration substrate. In *hmcn2/fbln1* double morphants, mesenchymal cells display reduced association with actinotrichia (Fig. 5F), reduced cell protrusion persistency (Fig. 4F) and reduced cell migration. Our cell autonomy (Fig. 4G,H) and Hmcn2 localization analyses (Fig. 1M) further indicate that this conditioning of the migratory substrate does not occur in a pericellular fashion, but spreads beyond individual Hmcn2/Fbln1-generating fin mesenchymal cells. This is consistent with findings in *C. elegans,* according to which Hmcn can move rather long distances within the embryo (Vogel and Hedgecock, 2001; Vogel et al., 2006).

In addition to the attachment between actinotrichia and mesenchymal cell protrusions, we found zebrafish Hmcn2 to be involved in the reorganization of the interepidermal cross fibers, which run perpendicular to the actinotrichia and are supposed to keep the two epidermal sheets together, involving the function of Hmcn1 (see above). In wild-type embryos, continuous cross fibers spanning the entire interepidermal space are only present in apical/distal regions (Fig. 5C), while more proximally -but still distal of the first mesenchymal cell protrusions - they start to rearrange into bouquet-like bundles (Figs. 5E and 6). Hmcn2 seems to be involved in this rearrangement, as cross fibers maintain a more distal-like organization throughout the entire proximodistal length of the fin fold (Fig. 5D). In this respect, Hmcn2 secreted by mesenchymal cells appears to modulate the spatial organisation of ECM structures that had been set up with the help of its close relative Hmcn1 secreted by apical epidermal cells. In light of the tight attachment between mesenchymal cells protrusions and cross fibers observed in *hmcn2/fbln1* double morphants (Fig. 5F,H), it is tempting to speculate that similar to the proposed function of Hmcn during male gonad development, allowing adjacent tissues to glide past each other (Vogel and Hedgecock, 2001; Vogel et al., 2006), zebrafish Hmcn2 might act as a kind of lubricant between cross fibers and mesenchymal cell protrusions to allow proper navigation of mesenchmyal cell protrusion between the cross fibers and through the subepidermal space.

Hemicentin 2 acts in functional redundancy with Fibulin 1

In contrast to Hmcn1, even complete knockdown of Hmcn2, as judged by absence of detectable protein via IHC, does not lead to any discernible phenotype, indicating that Hmcn2 per se is dispensable for zebrafish development. *hmcn2* MOs also failed to strengthen the defects of *hmcn1* mutants, suggesting that Hmcn2 does not act in functional redundancy with its direct paralogue, and consistent with their largely complementary expression patterns (Figure 1). However, Hmcn2 shares functions with Fibulin 1 (Fbln1), such that *hmcn2/fbln1* double morphant embryos display defects (see above) neither observed in *hmcn2* nor in *fbln1* single morphants, consistent with *hmcn2* and *fbln1* co-expression in affected embryonic structures (Figure 1).

Fibulin 1 is the founding member of the Fibulin family of ECM proteins (Argraves et al., 1989). In mammals, seven members of this family have been described, with Hmcn1 referred to as Fibulin 6 (Argraves et al., 2003; de Vega et al., 2009). However, we strongly believe that Hmcn2 should also be included, which would make a total of eight members. All of them share a stretch of EGF motifs followed by a globular FC domain in the C-terminal region, whereas the N-terminal regions of Fibulin 1 and Hemicentins are highly diverse (de Vega et al., 2009).

Compared to Hemicentins, the roles of Fibulin 1 during vertebrate development have been well studied. It is present in some BMs, in blood vessel walls and in multiple connective tissues, where it is often associated with microfibrils and elastic fibers (de Vega et al., 2009). Fibulin 1 knockout mice have multiple defects, including compromised formation of renal glomeruli and lung alveoli, and irregularly shaped endothelial compartments (Cooley et al., 2008; Kostka et al., 2001), consistent with the irregularly patterned intersegmental vessels observed in our *fbln1* morphant zebrafish (Supplementary Fig. S4). Of note, neither mouse nor zebrafish embryos display endothelial *fbln1* expression during normal development (Zhang et al., 1997; Zhang et al., 1996), raising a question about the source of Fibulin 1 contributing to vascular development and integrity. In mouse, vascular defects could be related to the earlier expression of *Fbln1* in cephalic neural crest cells that contribute to the pericytes and vascular smooth muscle cells (Cooley et al., 2008). However, in zebrafish, intersomitic vessel defects of *fbln1* morphants can be detected before smooth muscle cells (called mural cells) appear during normal development (Santoro et al., 2009). Future studies have to reveal whether *fbln1* expression in the somitic (Figure 1) or ventral mesoderm (Zhang et al., 1997) might contribute to vessel development, and to which extent this might also apply to mice and other vertebrates.

Interestingly, of all vertebrate fibulins, only Hemicentin and Fibulin 1 are present in *C. elegans.* For Fibulin 1, structural conservation even extends to the Fbln1C and Fbln1D splice isoforms (Barth et al., 1998). Most strikingly, Hmcn and the two Fbln1 isoforms display specific interactions during multiple processes of nematode development (Muriel et al., 2005; Vogel et al., 2006). Immunohistochemistry revealed that Fbln1 and Hmcn co-localize at many embryonic structures, and that Fbln1 is required for proper localization of Hmcn and vice versa, whereas other associated ECM proteins are not affected, pointing to a specific interaction between Hmcn and Fbln1 (Muriel et al., 2005). Furthermore, shared as well as isoform-specific functions and interactions with Hmcn have been reported for *C. elegans* Fbln1C and Fbln1D (Hesselson and Kimble, 2006; Muriel et al., 2005; Vogel et al., 2006), similar to our findings of shared functions of zebrafish Flbn1C and Fbln1D in epidermal-dermal junction formation in the trunk, but their distinct functions during fin morphogenesis (Table 1). To our knowledge, no *C. elegans fbln1/hmcn* double mutants have been described as yet. In light of our data obtained in zebrafish, we would expect them to show additional or stronger defects in processes with redundant, rather than closely interactive functions of Hmcn and Fbln1. It is also noteworthy that no skin defects comparable to those of *fbln1/hmcn2* double morphant zebrafish were observed in *Fbln1* mutant mice, although Fbln1 is a prominent component of the mouse skin, possibly also pointing to functional redundancy with other fibulins present in the skin, such as Hemicentins (Xu et al., 2007).

In sum, data obtained in *C. elegans* and zebrafish suggest that the roles of Hemicentins and their interactions with Fibulin-1 and its splice variants have been highly conserved throughout evolution, while future studies have to reveal to which extent they play redundant roles in organisms other than the zebrafish.

Possible molecular mechanisms of Hemicentin function

Thus far, no physical binding partners of Hemincentin proteins have been described (de Vega et al., 2009). Therefore, we can only speculate about the molecular basis of their functions during adhesiveness and cell migration. In *C. elegans,* Hmcn protein can assemble into linear tracks connecting adjacent cells, tissues or their respective BMs. Expression studies of different Hmcn domains as GFP-tagged fusion proteins have revealed that the N-terminal VWA domain targets the protein to multiple assembly sites, while the C-terminal EGF-FC modules mediates direct homophilic interaction between Hmcn momomers during track formation (Dong et al., 2006). It has been speculated that these tracks might constitute

elastic fiber-like structures, which are the precursors of the elastic fibers found in vertebrates (Vogel et al., 2006). Vertebrate elastic fibers consist of a core of polymerized fibrillin molecules, modified by the binding of elastin and several other associated proteins, including Fibulins (Ramirez and Sakai, 2010). Indeed, Fibulin-2, -4 and -5 have been shown to physically bind the microfiber core protein Fibrillin-1 (El-Hallous et al., 2007; Reinhardt et al., 1996). Since these fibulin members only have the C-terminal EGF-FC modules in common, it seems likely that bindung occurs via this region, which is also present in Hemicentins (de Vega et al., 2009). Therefore, it is tempting to speculate that zebrafish Fbln1 and Hmcn2 might also bind to Fibrillins, the possible constitutents of the fin fold cross fibers (see above). However, according to our anti-Hmcn2 immunohistological analyses, Hmcn2 protein is most prominent in the immediate subepidermal regions (Fig. 1M). Therefore, Hmcn2 and Flbn1 might not necessarily be global regulators of cross fiber integrity, but might rather modulate the (Hmcn1-dependent; see above) anchorage of cross fibers either to the BM or to the basal surface of basal keratinocytes. In line with this notion, we have preliminary data pointing to a direct physcial binding between Hmcn1/Hmcn2 and the BM component Nidogen (J.Z. and M.H., unpublished observations). In addition to cross fiber rearrangements, such interactions with BM components could also account for the observed compromised epidermal-dermal junction formation observed in the trunk (Figure 2) and, to a lower extent, in the fin folds (Figure 3K) of *hmcn2/fbln1* double morphant embryos. However, it seems unlikely that BM interactions also account for the effect of Hmcn2/Fbln1 on the attachment of fin mesenchymal cells to their migratory substrate, the actinotrichia, as this attachment takes place on the side of the actinotrichia facing away from the BM (see Figure 6). Actinotrichia-mesenchymal cell attachments could be mediated by direct binding between collagen type I/II proteins, the major constitutents of the actinotrichia (Duran et al., 2011), and integrin α2β1 receptors (Jokinen et al., 2004) at the surface of invading fin mesenchymal cells. However, it remains unclear how Hmcn2/Fbln1 could interfere with this binding, since apart from Collagen type XVIII, which is a non-fibrillar molecule found in BMs (Sasaki et al., 1998), no physical binding between Fibulin-1 and any collagens has been reported (de Vega et al., 2009).

In conclusion, this work identifies the thus far functionally uncharacterized vertebrate ECM protein Hmcn2 as a close and evolutionary conserved partner of Fibulin 1 during the regulation of different aspects of tissue adhesion and cell migration, thereby also extending current knowledge of Fibulin 1 functions (de Vega et al., 2009). In addition, it sheds first light on the ultrastructural basis of these in vivo functions, while further studies will be necessary to unravel the underlying molecular mechanisms.

Supplementary Material

Refer to Web version on PubMed Central for supplementary material.

Acknowledgments

We thank Mojgan Ghilav and Heike Wessendorf for expert technical assistance, and Dr. Hans-Martin Pogoda and Iris Riedl-Quinkertz for experiments during the revision of the manuscript. Work in the laboratory of MH was supported by the German Research Foundation (DFG; SFB 572; SFB 829 and its Z2 project), the European Union (Seventh Framework Programme, Integrated Project ZF-HEALTH, EC Grant Agreement HEALTH-F4-2010-242048) and the US National Institute of General Medical Sciences (GM63904). TJC's and VK's laboratories at the IMCB are supported by Agency for Science, Technology and Research (A-STAR) of Singapore.

References

Argraves WS, Dickerson K, Burgess WH, Ruoslahti E. Fibulin, a novel protein that interacts with the fibronectin receptor beta subunit cytoplasmic domain. Cell. 1989; 58:623–629. [PubMed: 2527614]

Argraves WS, Greene LM, Cooley MA, Gallagher WM. Fibulins: physiological and disease perspectives. EMBO Rep. 2003; 4:1127–1131. [PubMed: 14647206]

Argraves WS, Tran H, Burgess WH, Dickerson K. Fibulin is an extracellular matrix and plasma glycoprotein with repeated domain structure. J Cell Biol. 1990; 111:3155–3164. [PubMed: 2269669]

Balbona K, Tran H, Godyna S, Ingham KC, Strickland DK, Argraves WS. Fibulin binds to itself and to the carboxyl-terminal heparin-binding region of fibronectin. J Biol Chem. 1992; 267:20120–20125. [PubMed: 1400330]

Barth JL, Argraves KM, Roark EF, Little CD, Argraves WS. Identification of chicken and C. elegans fibulin-1 homologs and characterization of the C. elegans fibulin-1 gene. Matrix Biol. 1998; 17:635–646. [PubMed: 9923656]

Carney TJ, Feitosa NM, Sonntag C, Slanchev K, Kluger J, Kiyozumi D, Gebauer JM, Coffin Talbot J, Kimmel CB, Sekiguchi K, Wagener R, Schwarz H, Ingham PW, Hammerschmidt M. Genetic analysis of fin development in zebrafish identifies furin and hemicentin1 as potential novel fraser syndrome disease genes. PLoS Genet. 2010; 6:e1000907. [PubMed: 20419147]

Choo BG, Kondrichin I, Parinov S, Emelyanov A, Go W, Toh WC, Korzh V. Zebrafish transgenic Enhancer TRAP line database (ZETRAP). BMC Dev Biol. 2006; 6:5. [PubMed: 16478534]

Cooley MA, Kern CB, Fresco VM, Wessels A, Thompson RP, McQuinn TC, Twal WO, Mjaatvedt CH, Drake CJ, Argraves WS. Fibulin-1 is required for morphogenesis of neural crest-derived structures. Dev Biol. 2008; 319:336–345. [PubMed: 18538758]

Dane PJ, Tucker JB. Modulation of epidermal cell shaping and extracellular matrix during caudal fin morphogenesis in the zebra fish Brachydanio rerio. J Embryol Exp Morphol. 1985; 87:145–161. [PubMed: 4031750]

de Vega S, Iwamoto T, Yamada Y. Fibulins: multiple roles in matrix structures and tissue functions. Cell Mol Life Sci. 2009; 66:1890–1902. [PubMed: 19189051]

Dong C, Muriel JM, Ramirez S, Hutter H, Hedgecock EM, Breydo L, Baskakov IV, Vogel BE. Hemicentin assembly in the extracellular matrix is mediated by distinct structural modules. J Biol Chem. 2006; 281:23606–23610. [PubMed: 16798744]

Duran I, Mari-Beffa M, Santamaria JA, Becerra J, Santos-Ruiz L. Actinotrichia collagens and their role in fin formation. Dev Biol. 2011; 354:160–172. [PubMed: 21420398]

El-Hallous E, Sasaki T, Hubmacher D, Getie M, Tiedemann K, Brinckmann J, Batge B, Davis EC, Reinhardt DP. Fibrillin-1 interactions with fibulins depend on the first hybrid domain and provide an adaptor function to tropoelastin. J Biol Chem. 2007; 282:8935–8946. [PubMed: 17255108]

Feitosa NM, Richardson R, Bloch W, Hammerschmidt M. Basement membrane diseases in zebrafish. Methods Cell Biol. 2011; 105:191–222. [PubMed: 21951531]

Gansner JM, Madsen EC, Mecham RP, Gitlin JD. Essential role for fibrillin-2 in zebrafish notochord and vascular morphogenesis. Dev Dyn. 2008b; 237:2844–2861. [PubMed: 18816837]

Hammerschmidt M, Pelegri F, Mullins MC, Kane DA, van Eeden FJ, Granato M, Brand M, Furutani-Seiki M, Haffter P, Heisenberg CP, Jiang YJ, Kelsh RN, Odenthal J, Warga RM, Nusslein-Volhard C. dino and mercedes, two genes regulating dorsal development in the zebrafish embryo. Development. 1996; 123:95–102. [PubMed: 9007232]

Hesselson D, Kimble J. Growth control by EGF repeats of the C. elegans Fibulin-1C isoform. J Cell Biol. 2006; 175:217–223. [PubMed: 17043142]

Hopf M, Gohring W, Ries A, Timpl R, Hohenester E. Crystal structure and mutational analysis of a perlecan-binding fragment of nidogen-1. Nat Struct Biol. 2001; 8:634–640. [PubMed: 11427896]

Jokinen J, Dadu E, Nykvist P, Kapyla J, White DJ, Ivaska J, Vehvilainen P, Reunanen H, Larjava H, Hakkinen L, Heino J. Integrin-mediated cell adhesion to type I collagen fibrils. J Biol Chem. 2004; 279:31956–31963. [PubMed: 15145957]

Kimmel CB, Ballard WW, Kimmel SR, Ullmann B, Schilling TF. Stages of embryonic development of the zebrafish. Dev Dyn. 1995; 203:253–310. [PubMed: 8589427]

Kostka G, Giltay R, Bloch W, Addicks K, Timpl R, Fassler R, Chu ML. Perinatal lethality and endothelial cell abnormalities in several vessel compartments of fibulin-1-deficient mice. Mol Cell Biol. 2001; 21:7025–7034. [PubMed: 11564885]

Kubota Y, Kuroki R, Nishiwaki K. A fibulin-1 homolog interacts with an ADAM protease that controls cell migration in C. elegans. Curr Biol. 2004; 14:2011–2018. [PubMed: 15556863]

Lawson ND, Weinstein BM. In vivo imaging of embryonic vascular development using transgenic zebrafish. Dev Biol. 2002; 248:307–318. [PubMed: 12167406]

Le Guellec D, Morvan-Dubois G, Sire JY. Skin development in bony fish with particular emphasis on collagen deposition in the dermis of the zebrafish (Danio rerio). Int J Dev Biol. 2004; 48:217–231. [PubMed: 15272388]

Maertens B, Hopkins D, Franzke CW, Keene DR, Bruckner-Tuderman L, Greenspan DS, Koch M. Cleavage and oligomerization of gliomedin, a transmembrane collagen required for node of ranvier formation. J Biol Chem. 2007; 282:10647–10659. [PubMed: 17293346]

McGregor L, Makela V, Darling SM, Vrontou S, Chalepakis G, Roberts C, Smart N, Rutland P, Prescott N, Hopkins J, Bentley E, Shaw A, Roberts E, Mueller R, Jadeja S, Philip N, Nelson J, Francannet C, Perez-Aytes A, Megarbane A, Kerr B, Wainwright B, Woolf AS, Winter RM, Scambler PJ. Fraser syndrome and mouse blebbed phenotype caused by mutations in FRAS1/Fras1 encoding a putative extracellular matrix protein. Nat Genet. 2003; 34:203–208. [PubMed: 12766769]

Moon A, Yong HY, Song JI, Cukovic D, Salagrama S, Kaplan D, Putt D, Kim H, Dombkowski A, Kim HR. Global gene expression profiling unveils S100A8/A9 as candidate markers in H-ras-mediated human breast epithelial cell invasion. Mol Cancer Res. 2008; 6:1544–1553. [PubMed: 18922970]

Muriel JM, Dong C, Hutter H, Vogel BE. Fibulin-1C and Fibulin-1D splice variants have distinct functions and assemble in a hemicentin-dependent manner. Development. 2005; 132:4223–4234. [PubMed: 16120639]

Nasevicius A, Ekker SC. Effective targeted gene 'knockdown' in zebrafish. Nat Genet. 2000; 26:216–220. [PubMed: 11017081]

Nüsslein-Volhard, C.; Dahm, R. Zebrafish: a Practical Approach. Oxford University Press; New York: 2002.

Pan TC, Kluge M, Zhang RZ, Mayer U, Timpl R, Chu ML. Sequence of extracellular mouse protein BM-90/fibulin and its calcium-dependent binding to other basement-membrane ligands. Eur J Biochem. 1993; 215:733–740. [PubMed: 8354280]

Perbal B, Martinerie C, Sainson R, Werner M, He B, Roizman B. The C-terminal domain of the regulatory protein NOVH is sufficient to promote interaction with fibulin 1C: a clue for a role of NOVH in cell-adhesion signaling. Proc Natl Acad Sci U S A. 1999; 96:869–874. [PubMed: 9927660]

Ramirez F, Sakai LY. Biogenesis and function of fibrillin assemblies. Cell Tissue Res. 2010; 339:71–82. [PubMed: 19513754]

Reinhardt DP, Sasaki T, Dzamba BJ, Keene DR, Chu ML, Gohring W, Timpl R, Sakai LY. Fibrillin-1 and fibulin-2 interact and are colocalized in some tissues. J Biol Chem. 1996; 271:19489–19496. [PubMed: 8702639]

Santoro MM, Pesce G, Stainier DY. Characterization of vascular mural cells during zebrafish development. Mech Dev. 2009; 126:638–649. [PubMed: 19539756]

Sasaki T, Fukai N, Mann K, Gohring W, Olsen BR, Timpl R. Structure, function and tissue forms of the C-terminal globular domain of collagen XVIII containing the angiogenesis inhibitor endostatin. Embo J. 1998; 17:4249–4256. [PubMed: 9687493]

Sasaki T, Kostka G, Gohring W, Wiedemann H, Mann K, Chu ML, Timpl R. Structural characterization of two variants of fibulin-1 that differ in nidogen affinity. J Mol Biol. 1995; 245:241–250. [PubMed: 7844816]

Schulte-Merker S, Ho RK, Herrmann BG, Nusslein-Volhard C. The protein product of the zebrafish homologue of the mouse T gene is expressed in nuclei of the germ ring and the notochord of the early embryo. Development. 1992; 116:1021–1032. [PubMed: 1295726]

Sherwood DR. Cell invasion through basement membranes: an anchor of understanding. Trends Cell Biol. 2006; 16:250–256. [PubMed: 16580836]

Sherwood DR, Butler JA, Kramer JM, Sternberg PW. FOS-1 promotes basement-membrane removal during anchor-cell invasion in C. elegans. Cell. 2005; 121:951–962. [PubMed: 15960981]

Smyth I, Scambler P. The genetics of Fraser syndrome and the blebs mouse mutants. Hum Mol Genet. 2005; 14(Spec No 2):R269–274. [PubMed: 16244325]

Tran H, VanDusen WJ, Argraves WS. The self-association and fibronectin-binding sites of fibulin-1 map to calcium-binding epidermal growth factor-like domains. J Biol Chem. 1997; 272:22600–22606. [PubMed: 9278415]

Twal WO, Czirok A, Hegedus B, Knaak C, Chintalapudi MR, Okagawa H, Sugi Y, Argraves WS. Fibulin-1 suppression of fibronectin-regulated cell adhesion and motility. J Cell Sci. 2001; 114:4587–4598. [PubMed: 11792823]

Vogel BE, Hedgecock EM. Hemicentin, a conserved extracellular member of the immunoglobulin superfamily, organizes epithelial and other cell attachments into oriented line-shaped junctions. Development. 2001; 128:883–894. [PubMed: 11222143]

Vogel BE, Muriel JM, Dong C, Xu X. Hemicentins: what have we learned from worms? Cell Res. 2006; 16:872–878. [PubMed: 17031392]

Vogel BE, Wagner C, Paterson JM, Xu X, Yanowitz JL. An extracellular matrix protein prevents cytokinesis failure and aneuploidy in the C. elegans germline. Cell Cycle. 2011; 10:1916–1920. [PubMed: 21558805]

Vrontou S, Petrou P, Meyer BI, Galanopoulos VK, Imai K, Yanagi M, Chowdhury K, Scambler PJ, Chalepakis G. Fras1 deficiency results in cryptophthalmos, renal agenesis and blebbed phenotype in mice. Nat Genet. 2003; 34:209–214. [PubMed: 12766770]

Wood A, Thorogood P. An analysis of in vivo cell migration during teleost fin morphogenesis. J Cell Sci. 1984; 66:205–222. [PubMed: 6746756]

Xu X, Dong C, Vogel BE. Hemicentins assemble on diverse epithelia in the mouse. J Histochem Cytochem. 2007; 55:119–126. [PubMed: 17015624]

Xu X, Vogel BE. A secreted protein promotes cleavage furrow maturation during cytokinesis. Curr Biol. 2011; 21:114–119. [PubMed: 21215633]

Zhang HY, Lardelli M, Ekblom P. Sequence of zebrafish fibulin-1 and its expression in developing heart and other embryonic organs. Dev Genes Evol. 1997; 207(5):340–351.

Zhang HY, Timpl R, Sasaki T, Chu ML, Ekblom P. Fibulin-1 and fibulin-2 expression during organogenesis in the developing mouse embryo. Dev Dyn. 1996; 205:348–364. [PubMed: 8850569]

Zhang J, Wagh P, Guay D, Sanchez-Pulido L, Padhi BK, Korzh V, Andrade-Navarro MA, Akimenko MA. Loss of fish actinotrichia proteins and the fin-to-limb transition. Nature. 2010; 466:234–237. [PubMed: 20574421]

Highlights

- First analysis of Hmcn2 function in vertebrates
- Hmcn2 acts in partial functional redundancy with Fibulin 1
- Hmcn2/Fbln1 from internal sources regulate epidermal-dermal junction formation
- Hmcn2/Fbln1-dependent ECM remodelling is required for mesenchymal cell migration
- Tight interaction between Hmcn2 and Fbln1 is evolutionary highly conserved

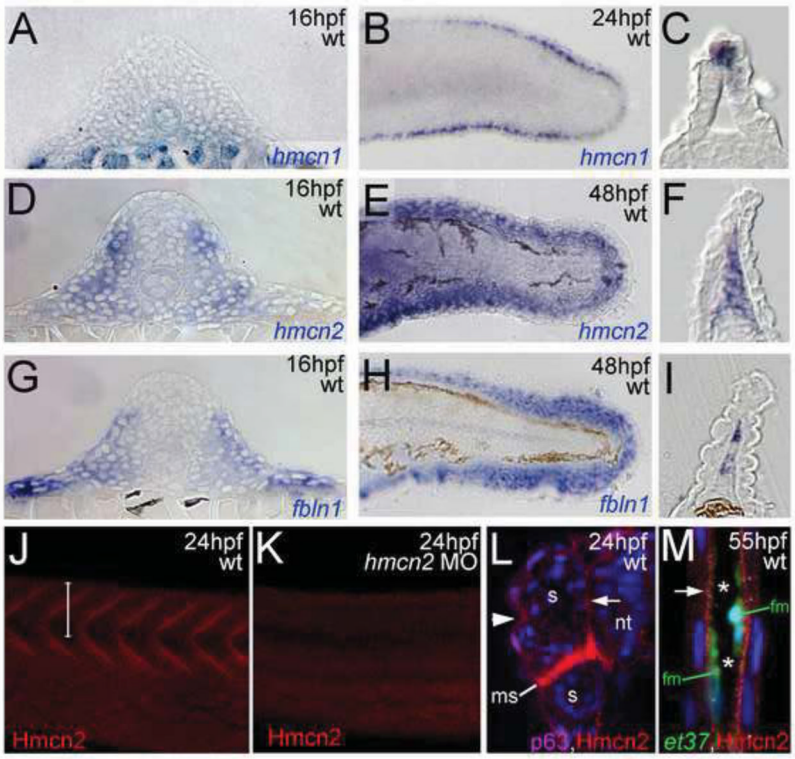

Figure 1. *hmcn2* and *fbln1* are co-expressed in somites and fin mesenchymal cells

(A–I) in situ hybridizations with probes indicated lower right corners; (A,D,G) transverse sections through trunk at 14 hpf (14 somite stage); (B,E,H) lateral view on tail at 24 hpf (B) or 48 hpf (E,H); (C,F,I) transverse sections through tail of embryos as shown in (B,E,H), respectively; view on dorsal median fin fold. (A,D,G) *hmcn2* (D) and *fbln1* (G) are co-expressed in somites, whereas *hmcn1* (A) is not. (B,C,E,F,H,I) *hmcn1* (B,C) is expressed in epidermal cells at the apical ridge of the fin fold, while *hmcn2* (E,F) and *fbln1* (H,I) are expressed in fin mesenchymal cells within the dermal (interepidermal) space of the fin fold. (J–M) Anti-Hmcn2 immunostainings. (J,K) Lateral view on trunk at 24 hpf, revealing Hmcn2 protein at myosepta of uninjected control-(J), whereas myoseptal staining is absent in *hmcn2* morphant (K). (L) Transverse section through 24 hpf wild-type embryo at level indicated in (J). counterstained with anti-p63 antibody to stain nuclei of basal keratinocytes, and DAPI to visualize all nuclei. Arrowhead points to Hmcn2 protein in dermal space between epidermis and somites, arrow to Hmcn2 protein between neural tube and somites. (M) Transverse section through dorsal fin at 55 hpf embryo, showing Hmcn2 protein in red, mesenchymal cells in green (anti-GFP of ET37 transgene product), and DAPI-positive nuclei in blue. Hmcn2 protein is present in continuous lines below the epidermal sheets (blue nuclei). Strikingly, Hmcn2 protein is not restricted to regions that contain fin mesenchymal cells and their protrusions (in green), but also found in more apical regions (indicated by arrow), in line with its non-pericellular function during the guidance of mesenchymal cell migration described below (Figure 4). However, inner regions of the dermal space of the fin lack Hmcn2 signals (indicated by stars).

Abbreviations: wt, wild type; hmcn2 MO, hmcn2 morphant; hpf, hours post fertilization; ms, horizontal myoseptum; nt, neural tube; s, somite.

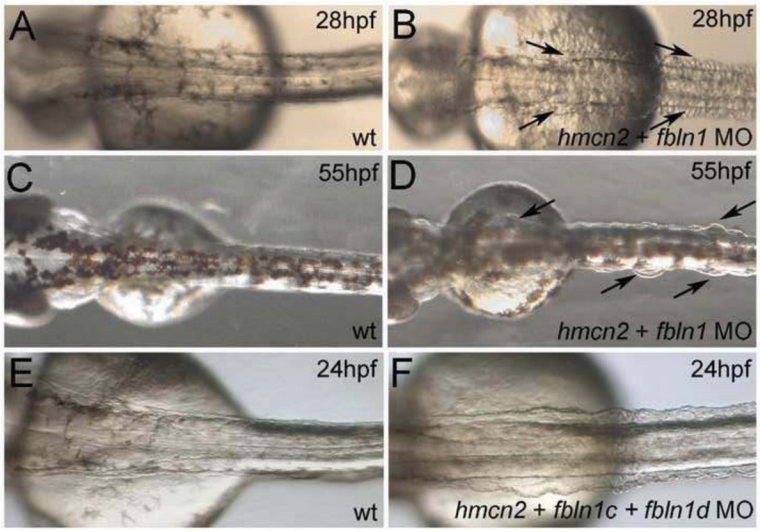

Figure 2. *hmcn2/fbln1* double morphants display trunk blistering

Dorsal views on the trunk and tail of live embryos at stages indicated in upper right corners; anterior to the right. Arrows in embryos co-injected with *hmcn2* MO and translation-blocking *fbln1* MO in (B,D) point to blisters that are massive and widespread at 28 hpf (B), but alleviated and more locally restricted at 55 hpf (D). (E,F) Severe blistering is also obtained upon co-injection of *hmcn2* MO with MOs targeting the two Fbln1 splice variants *(fbln1c +fbln1d).*

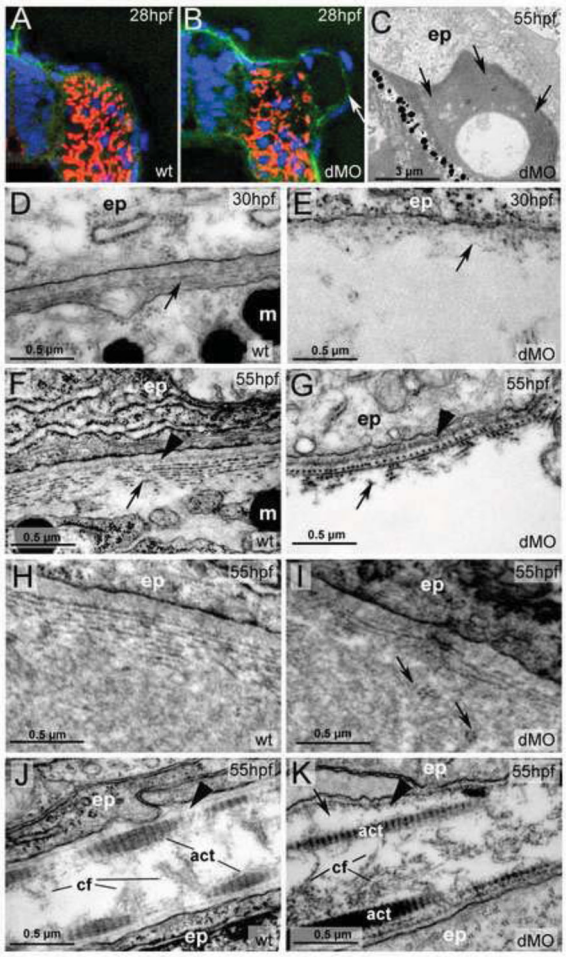

Figure 3. *hmcn2/fbln1* double morphants display strongly compromised epidermal-dermal junction formation in the trunk, but not in the fin fold

(A,B) Transverse sections through trunk at 28 hpf, after anti-Laminin immunolabelling of BMs in green, Phalloidin-labelling of somitic muscle in red, and DAPI labelling of nuclei in blue. The double morphant (B) displays Laminin labelling at both sides of the blister, indicating that both epidermis and somites are properly attached to their respective basement membranes, and that blistering occurs within the dermal space in between.

(C–K) Transmission electron micrographs of transverse sections through trunk (C–I) or dorsal tail fin (J.K) at stages indicated in upper right corners (for magnification, see scale bars).

(C) Double morphant at low magnification, with most of trunk blister filled with amorphic material at 55 hpf. (D,E) At 30 hpf, wild-type embryo (D) displays the first collagen fibers (arrow) underneath the yet indistinct BM, whereas much fewer fibers are present in the double morphant, with a fluid-filled blister underneath (E). Thinner and short fibers possibly integrated into and running perpendicular to the BM are visible in the double morphant (E; arrow), but more difficult to see in the wild-type (D,F), most likely due to the more compact organization of the tissue. It is tempting to speculate that they are the equivalent of the cross fibers of the fin fold (see Figure 5), and involved in the organization of the ECM across the dermal space. (F,G) At 55 hpf, the collagenous network underneath the BM of the wild-type embryo consists of approximately ten layers organized in a plywood-like fasion (F), whereas the double morphant embryo displays a rupture within the second and third collagen layer (G). The shown specimen is one of the rare cases in which the blister seems to remain fluid-

filled (see below). Arrowheads point to BMs. (H,I) In regions in which the architecture of the wild-type embryo requires a wider dermal space, such as at the base of the fins, it is filled with amorphic material underneath the sublaminal collagen fibers (H). In double morphants (I), most trunk blisters are filled with similar amorphic material, intermingled by disorganized and not properly anchored collagen fibers (arrows).

(J,K) In the fin fold of wild-type embryos (J), collagenous actinotrichia are attached to the BM (indicated by arrowhead). In double morphant (K), actinotrichia and BM (indicated by arrowhead) appear unaffected, with rare and locally restricted detachments (indicated by arrow) in medio-basal regions of the fin.

Abbreviations: act, actinotrichia; cf, cross fibers; dMO, double morphant; ep, epidermal cell; m, melanocyte

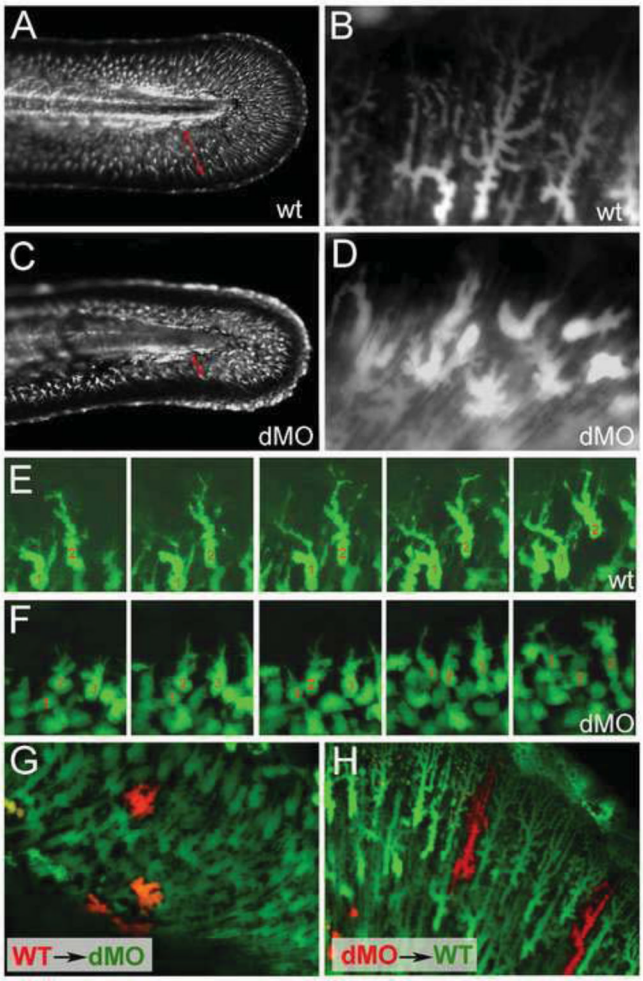

Figure 4. *hmcn2/fbln1* double morphants display non-cell autonomous defects in fin mesenchymal cell migration

All panels show lateral views on the tail of live ET37 transgenic embryos, in which fin mesenchymal cells express GFP. (A–D) Overview (A,C) and magnified view of same embryos (B,D) at 55 hpf. Red arrows in (A,C) indicate the distance between the leading edge of in mesenchymal cells and the base of the dorsal median fin, which is strongly reduced in the double morphant (C). Note that in the double morphant (C), the apical regions of the fin are collapsed, most likely as a secondary consequence of impaired mesenchymal cell immigration. Magnified views (B,D), showing that in wild-type embryo (B), fin mesenchymal cells have long protrusions that project laterally and apically (distally), whereas in the double morphant (D) cells have a more roundish shape with shorter and thicker protrusions.

(E,F) Stills from time-lapse recordings of fin mesenchymal cells of wild-type (E) and double morphant embryo (F) from 35 – 40 hpf; individual cells are marked by numbers. (E) In wild-type, mesenchymal cells make stable protrusions that extend apically, followed by a displacemnt of the cell body into the same direction. (F) In the double morphant mesenchymal cells do form protrusions, however, protrusion are shorter and less persistent, and often (cell 2), but not always (cell 1), retract without cell body displacement. (G,H) Chimeric embryos at 72 hpf, generated via cell transplantations at early gastrula stage (6 hpf). (G) In double morphant host, wild-type mesenchymal cells (red) show compromised migratory behavior and cell shapes like their double morphant neighbors (green). (H) In

wild-type host, double morphant mesenchymal cells (red) display highly arborized cells shapes like their wild-type neighbors (green), and can be found at the leading edge of the ingrowth, pointing to uncompromised migratory behavior.

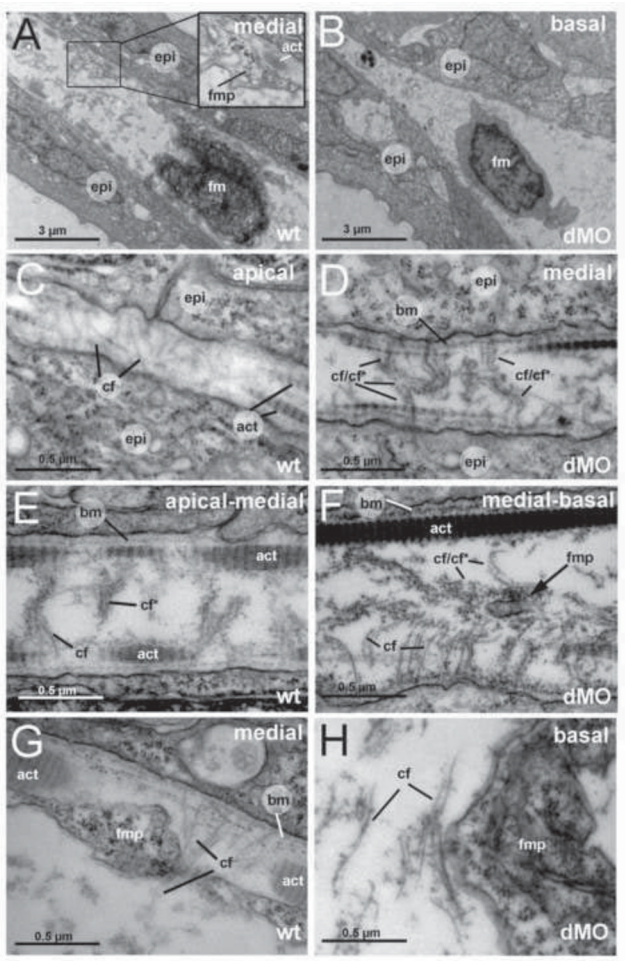

Figure 5. The fin folds of *hmcn2/fbln1* double morphants display compromised cross fiber rearrangements and aberrant detachments of fin mesenchymal protrusions from collagenous actinotrichia

All panels show transmission electron micrographs of transverse sections through the dorsal median fin at 55 hpf. Positions of sections along the apical-basal (distal-proximal) axis of the fin are indicated in upper right corners. See scale bars for magnifications. (A,C,E,G) wild type; (B,D,F,H) *hmcn2/fbln1* double morphant. (A) In wild-type embryo the mesenchymal cell is located in a medial region of the fin and has long projections that align along the actinotrichia (inset with magnification), projecting apically. (B) In double morphant, the space between the two epidermal sheets is very narrow, and the mesenchymal cell body is located in basal regions of the fin. (C) In apical-most regions of the wild-type fin, numerous cross fibers (cf) span the entire dermal space in parallel bundles and at right angles to the actinotrichia (act), connecting to the apposed epithelial sheets. (E) In apical-medial regions, but still apical of the fin mesenchymal cells and their protrusions, cross fibers display a bouquet-like organization in regions close to the cell surfaces and actinotrichia (cf), while in central regions of the dermal space, they are decorated by electron-dense material (cf*). (G) In medial regions, protrusions of fin mesenchymal cells are attached to the inner surface of the actinotrichia, while weaving between the cross fiber bouquets. (D) Medial fin regions of *hmcn2/fbln1* double morphants (D) display an organization of cross fibers similar to that of apical-most regions of wild-type fins (compare with C), with cross fibers spanning the entire dermal space. (F) The few protrusion of fin mesenchymal cells that make it into basal-medial positions are not attached to the

actinotrichia as in wild type, although actinotrichia of are normal thickness and pattern (compare with E), but found in central regions of the dermal space, surrounded by cross fibers. (G) Aberrant tight attachments between fin mesenchymal cells and cross fibers are also observed in the fin base of *hmcn2/fbln1* double morphants.
Abbreviations: act, actinotrichia; cf, cross fiber; cf*, decorated cross fiber; ep, epidermis; fm, fin mesenchymal cell; fmp, fin mesenchymal cell protrusion.

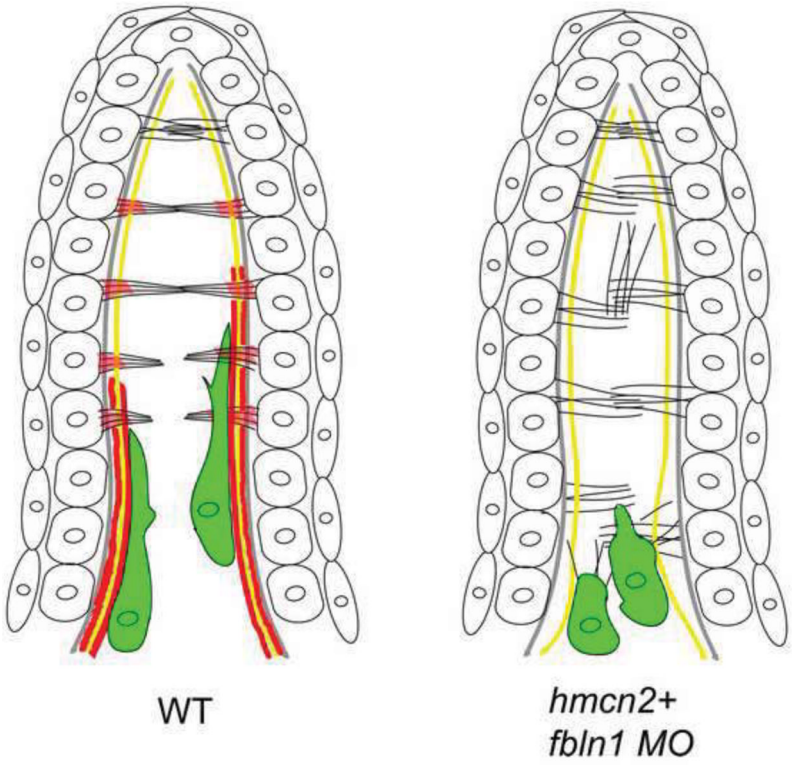

Figure 6. Simplified diagram illustrating the organization of the dorsal median fin fold in wild-type and *hmcn2/fbln1* double morphant embryos at 55 hpf

The cartoon shows the bilayered epidermal sheets, the epidermal BM in grey, actinotrichia in yellow, cross fibers in black, and fin mesenchymal cells in green. In red are the sites of Hmcn2/Fbln1 action, based on mutant analyses and anti-Hmcn2 immunohistochemistry. For simplicity, only some cross fibers are shown.

Left panel: in wild-type embryos, the cross fibers in the apical-most regions of the fin fold run in parallel and perpendicular to actinotrichia, spanning the entire interepidermal space, while in medial regions, they display a bouquet-like organization, possibly mediated by Hmcn2 located in subepidermal regions. Fin mesenchymal cells migrate on the inner surface of actinotrichia, weaving between the cross fibers. It is currently unclear whether this is directly mediated by Hmcn2 bound to actinotrichia or due to indirect effects (see Discussion).

Right panel: in the absence of Hmcn2 and Fbln1, cross fibers throughout the entire length of the fin fold remain in an organization more reminiscent of apical-most regions in wild type. The mesenchymal cells fail to migrate along the actinotrichia and remain at the base of the fin, “trapped” within cross fibers.

Table 1

Phenotypes obtained upon single or double injections of different *hmcn2* and *fbln1* morpholinos

stage	30hpf		55hpf		
Phenotype / **MO**	**Blisters trunk**	**n**	**Blisters trunk**	**Fin defect**	**n**
hmcn2 0.5 mM	0%	163	0%	0%	163
fbln1 0.1 mM	0%	176	0%	0%	176
fbln1c 0.125 mM	0%	97	0%	0%	97
fbln1d 0.125 mM	0%	98	0%	0%	98
hmcn2 0.5mM + *fbln1* 0.1 mM	60,4%	447	37%	62,7%	243
hmcn2 0.5 mM + *fbln1c* 0.125 mM	0%	93	0%	74,2%	93
hmcn2 0.5 mM + *fbln1d* 0.125 mM	0%	120	0%	63,3%	120
hmcn2 0.5 mM + *fbln1c* 0.125 mM + *fbln1d* 0.125 mM	61,3%	132	41%	84,8%	132

Defects were analyzed via light microscopy at indicated stages. The reduction of trunk blistering frequency from 30 hpf to 55 hpf is caused by progressive healing of this phenotypic trait (see Figure 2 and Supplementary Fig. S5C,E for 72 hpf), whereas fin defects persist (see Supplementary Fig. S5D,F for 72 hpf). For testing of Fbln1 splice variants, note that fin defects were obtained both upon co-injection of *fbln1c* and *hmcn2* MOs, and upon co-injection of *fbln1d* and *hmcn2* MOs, whereas trunk blistering required triple injection of *fbln1c, fbln1d* and *hmcn2* MOs. n, number of scored embryos (3 independent experiments).